Bioresource Technology Reports 17 (2022) 100911

Contents lists available at ScienceDirect

Bioresource Technology Reports

journal homepage: www.sciencedirect.com/journal/bioresource-technology-reports

Microbial lignin degradation in an industrial composting environment

Katharina Duran [a], Marijn van den Dikkenberg [a], Gijs van Erven [a,b], Johan J.P. Baars [c], Rob N. J. Comans [d], Thomas W. Kuyper [e], Mirjam A. Kabel [a,*]

[a] Laboratory of Food Chemistry, Wageningen University & Research, Bornse Weilanden 9, 6708 WG Wageningen, the Netherlands
[b] Wageningen Food & Biobased Research, Bornse Weilanden 9, 6708 WG Wageningen, the Netherlands
[c] CNC Grondstoffen, Driekronenstraat 6, 6596 MA Milsbeek, the Netherlands
[d] Soil Chemistry and Chemical Soil Quality Group, Wageningen University & Research, Droevendaalsesteeg 3a, 6708 PB Wageningen, the Netherlands
[e] Soil Biology Group, Wageningen University & Research, Droevendaalsesteeg 3, 6700 AA Wageningen, the Netherlands

ARTICLE INFO

Keywords:
Lignin
Pyrolysis-GC–MS
^{13}C isotope labelling
Microbial delignification
Composting

ABSTRACT

Composting is an essential biochemical process to pre-treat lignocellulosic biomass (e.g., wheat straw) to generate nutritious substrate for industrial *Agaricus bisporus* production. During composting numerous microbes target (hemi-)cellulose using their enzymatic machinery, while lignin has been assumed to remain unaffected. This research aimed to unravel the chemical and microbial changes during a 4-day industrial composting process with special emphasis on the fate of lignin. A recently developed pyrolysis-GC–MS method using a ^{13}C-lignin isolate as internal standard enabled targeted quantitative lignin analysis. As previously demonstrated, a 40% w/w decrease in (hemi-)cellulose was observed, while unexpectedly lignin decreased by 30% w/w. Increased C_{α}-oxidized moieties and cleaved interunit linkages substantiated this lignin removal. Simultaneously, a microbial community shift towards Alphaproteobacteria, Gammaproteobacteria, Actinobacteria and Sordariomycetes occurred. Hence, the compost environment provided appropriate conditions to harbor a microbial community to alter and degrade lignin, and this research provides new insights into underlying lignin degradation mechanisms.

1. Introduction

In nature, decomposition of complex biomass is driving carbon cycling and enables the release and availability of nutrients. Adapted and inspired by these natural processes, composting aims to accelerate decomposition of complex, heterogenous organic waste streams in an artificial environment (Meghvansi and Varma, 2020). This process is exemplified by the conversion of carbon-rich agricultural by-products and nitrogen-rich animal stock waste streams into soil improvers, or to generate substrate for (industrial scale) mushroom cultivation (Bernal et al., 2009).

This research investigates a distinct microbial composting phase, named phase II (PII), of a white button mushroom (*Agaricus bisporus*) substrate production process. In brief, the overall industrial substrate production comprises a short thermophilic pretreatment (PI), a microbial composting phase (PII), a vegetative growth phase of *A. bisporus* (PIII), and a fruiting body formation phase (PIV) (for details see Kabel et al., 2017a). It has been well described that during PII a diverse microbial community degrades a recalcitrant lignocellulosic substrate (e.g., wheat straw), and drives the formation of a specific and selective substrate to be used for industrial cultivation of *A. bisporus* (Kertesz and Thai, 2018; Zhang et al., 2019). Still, a better understanding of PII and of the transformations the biomass undergoes will eventually help to optimize substrate usage. Products of microbial conversion and microbial biomass are a potential nutrient source for *A. bisporus* (Fermor et al., 1991). In this context, particularly Proteobacteria, Actinobacteria and Sordariomycetes have been identified (Bugg et al., 2020; Wang et al., 2016; Zhang et al., 2019).

The mushroom compost of this research is wheat straw based and consists of cell wall polysaccharides and lignin that are partly degraded during PII (Kabel et al., 2017). These polysaccharides comprise mainly of cellulose and hemicellulosic (glucuronoarabino-) xylan (GAX). Cellulose is exclusively composed of β-(1 → 4)-linked glucosyl units, while GAX has a backbone of β-(1 → 4)-linked xylopyranosyl units substituted with α-L-arabinofuranosyl units, (4-*O*-methyl-)glucuronosyl units and *O*-acetyl esters (Gírio et al., 2010). Lignin is a complex, heteroaromatic polymer, consisting of *p*-hydroxyphenyl (H), syringyl (S) and guaiacyl (G) units, with the *β-O-4′* aryl ether as most abundant interunit linkage

* Corresponding author.
E-mail address: mirjam.kabel@wur.nl (M.A. Kabel).

https://doi.org/10.1016/j.biteb.2021.100911
Received 11 October 2021; Received in revised form 1 December 2021; Accepted 7 December 2021
Available online 16 December 2021

(~75%) (Ralph et al., 2004). The carbohydrate (e.g., GAX and cellulose) degradation during PII (Jurak et al., 2015) is assumed to result from excreted enzymes by microbes in PII (Carrasco et al., 2020; Vieira and Pecchia, 2018). Indeed, xylan and cellulose degrading enzymes were annotated in compost material obtained in the end of PII in a previous proteome study. (Patyshakuliyeva et al., 2015).

However, many studies suggested that lignin resists degradation and remains unaltered during PII (Carrasco et al., 2020; Iiyama et al., 1994; Jurak et al., 2015; Zhang et al., 2019). It is important to note that lignin analysis so far relied on gravimetric and spectrophotometric methods known to be interfered by for example microbial biomass, which might have resulted in overestimation of lignin in compost and hence in underestimation of the lignin degradation potential (Carrasco et al., 2020; Iiyama et al., 1994; Zhang et al., 2019). Nonetheless, it has been described that lignin can be transformed during composting and structural alterations such as a decrease in S/G ratio, increase in aromaticity and carbonyl groups have been described (Albrecht et al., 2008; Chen et al., 1989). Those studies already indicated that lignin is not inert, although specific lignin quantification has remained a challenge (reviewed by Tuomela, 2000). In addition, microbes known to degrade and mineralize lignin, such as the Proteobacteria *Pseudomonas* sp. and *Sphingobium* sp. (Gall et al., 2014), have been reported to colonize the mushroom compost (Siyoum et al., 2016). Therefore, it is hypothesized here that lignin is altered and degraded throughout PII.

Additionally, during PII it has visually been observed that gradually a dark biofilm layer (DF) is formed on the surface of wheat straw (Iiyami et al., 1996). This DF formation might be linked to the net microbial biomass increase, and researchers have suggested its nutritive importance for *A. bisporus* (Wain, 1981). Knowing DF composition might help improve nutrient distribution for vegetative *A. bisporus* growth. In DF, microbial biomass and necromass, (partially degraded) wheat straw carbohydrates, and even lignin have been suggested to be present (Iiyami et al., 1996; Smith and Spencer, 1976). A complete and specific compositional analysis of DF remains elusive to date, as well as the fate and composition of lignin and its possible incorporation in DF. However, the suggestion that (degraded) lignin is present in DF (Iiyami et al., 1996) stands in contrast with the general assumption that lignin remains unaltered throughout PII.

To study the hypothesis that throughout PII composting microbial delignification takes place, and that lignin degradation products are partially incorporated in DF, compost and DF were sampled at five timepoints and mass yields were determined. In addition, carbohydrate, fatty acid, nitrogen and lignin contents and composition were analyzed. For specific lignin quantification a novel and recently developed pyrolysis-GC–MS method was applied, making use of a ^{13}C-lignin isolate as internal standard (^{13}C-IS py-GC–MS; van Erven et al., 2017). This state-of-the art method allows the specific quantification of lignin and concurrently provides structural insights. In addition, the compost and DF samples were semi-quantified for selected microbial targets related to compost quality by qPCR, while a more detailed microbial community composition was determined by 16S/18S rRNA sequencing. By combining data from both chemical and microbiological analyses this research provides a deeper understanding of the dynamic interplay between the microbiome and the chemical constituents of compost and DF and revisits the view that lignin is inert during PII composting.

2. Materials and Methods

2.1. Materials and chemicals

In December 2019 compost material was obtained from PII (see 2.2) of an industrial *A. bisporus* substrate production facility (CNC Grondstoffen (Milsbeek, The Netherlands)). Uniformly ^{13}C-labeled wheat straw lignin isolate (^{13}C-IS, 97.7 atom% ^{13}C), isolated from ^{13}C-wheat straw (IsoLife, Wageningen), was available from previous research (van Erven et al., 2017). Natural latex (polyisoprene) was purchased from Colok GmbH (Berlin, Germany). All other chemicals were of analytical grade and purchased from Sigma-Aldrich or Merck unless specified otherwise. Water was purified using a MilliQ system (Millipore, Billerica, MA, USA).

2.2. Sampling of PII compost and sample preparation

A PII tunnel was filled with compost material resulting from the first CNC-treatment phase (PI – material from two PI tunnels was combined) and mixed with 1% *w*/w of PII-end material to introduce a thermophilic microbial community (Jurak et al., 2015). Prior to filling of the PII tunnel, well mixed PI material was stored at −18 °C (C_{D0}). Next, 4 net-bags filled with PI compost (per bag 8 kg ± 10%) were burrowed into the compost material in the PII tunnel and each net-bag was equipped with a temperature logger (Sterildisk10, TService BV, Gennep, The Netherlands) to track the temperature changes in each individual bag (supplementary material). After the tunnel was closed, PII composting started, and after 19.5 h, 42.5 h, 66.5 h and 89.0 h one net-bag was collected through a folding hatch, and coded C_{D1}, C_{D2}, C_{D3} and C_{D4}, respectively. The PII tunnel was immediately emptied after collection of C_{D4}. The bags were weighed, and the compost was thoroughly mixed per bag. A part of the mixed compost was stored at −18 °C (C_{D0} - C_{D4}; about 1 kg per bag), a second part was lyophilized (1 kg (± 10%)) and a third part (1 kg (±10%)) was used to isolate dark film from (see 2.3). The mixed fresh compost samples were measured for pH and dry weight, ash, nitrogen (Kjeldahl) as previously described (Jurak et al., 2015). Lyophilized samples were milled (< 1 mm) using a MM 2000 mill (Retsch, Haan, Germany), and analyzed for ash, nitrogen (DUMAS), carbohydrates, used for DNA extraction and to extract water soluble material from. An aliquot of 2 g of milled material was further milled at 600 rpm with a planetary ball mill, PM 100 (Retsch, Haan, Germany), in a zirconium dioxide (ZrO_2) jar containing 17 ZrO_2 beads (φ 10 mm) for 30 min net milling and after each 10 min milling a 5 min break was held to prevent overheating. The planetary ball milled samples were used for lignin analysis with py-GC–MS and for fatty acid analysis.

2.3. Isolation of dark film from fresh PII compost

A novel mechanical dark film isolation protocol was developed to extract DF from fresh PII compost samples. Hereto, the bottom surface of a plastic container (22.7 cm width 32.7 cm length 6 cm height) was coated with liquid natural latex. The latex coating solidified at room temperature within 12 h and was rinsed with excess milliQ. About 15 g of fresh compost (C_{D0} to C_{D4}) were placed in the coated box together with 15 silicon dioxide (SiO_2) beads (φ 30 mm) and with a closed lid carefully manually shaken for 45 s. With a brush, wheat straw fibers sticking to the latex were removed and collected (remaining wheat-straw; R_{WSI}). Next, dark material adhering to the latex surface was suspended in 10 mL milliQ. The suspension of each isolation step was collected, pooled, lyophilized. The isolation steps were repeated 15–20 times and the isolated material was combined. In total 3 batches, of each 300 g, were processed per sample (C_{D0} to C_{D4}). Subsequently, the pooled lyophilized batches were sieved making use of two sieve sizes: 250 μm and 106 μm. The fractions >250 μm and 106–250 μm were abbreviated DF_{IRWS_1} and DF_{IRWS2} (dark film remaining wheat straw 1 and 2), respectively, and contained wheat straw fibers. The fraction that passed through both sieves was visually free of wheat straw fibers and this <106 μm fraction was defined as isolated dark film layer (DF_{D0} to DF_{D4}).

2.4. Water fractionation of lyophilized compost

Lyophilized and milled (< 1 mm) samples (5 g, C_{D0} to C_{D4}) were suspended in 175 mL preheated (100 °C) milliQ and boiled for 15 min in a water bath to inactivate microorganisms and enzymes. Next, suspensions were rotated end-over-end (40 rpm, 2 h, 65 °C), and the supernatants were collected after centrifugation (18,600 ×*g*, 0.5 h, 20 °C).

The residue was washed twice with milliQ (80 mL), centrifuged (18,600 ×*g*, 0.5 h, 20 °C) and all supernatants were pooled. An aliquot of 60 mL of pooled supernatant (SN) was filtered (Whatman, cellulose acetate, 0.2 μm pore size), freeze dried, coded SN_{D0} to SN_{D4}, and analyzed by ^{13}C-IS pyrolysis-GC–MS.

2.5. Cultivation of microbial controls (bacteria and fungi)

The thermophilic PII-fungus *Mycothermus thermophilus* and PII-bacteria were cultured, and their microbial biomass was used as reference and to cross-check the lignin, fatty acid and carbohydrate content and composition (supplementary material).

2.6. DNA extraction

DNA extraction of the dried, milled (< 1 mm) compost (C_{D0} to C_{D4}) (100 mg) in duplicate, and of dark film (250 mg), was performed using the DNeasy PowerSoil Kit (Qiagen, Hilden, Germany) according to the manufacturer's protocol.

2.7. Ash content

Samples were dried overnight at 105 °C and subjected for 4 h to 575 °C. The residue left after combusting at 575 °C is defined as ash.

2.8. Nitrogen content – by DUMAS

The total nitrogen content was measured by combustion on a Flash EA 1112 Nitrogen Analyzer (DUMAS) (Thermo Scientific, Sunnyvale, CA, USA). D-methionine was used for calibration.

2.9. Sugar content and composition

Neutral anhydrocarbohydrate content and composition was determined in duplicate according to the procedure described in supplementary material (Englyst and Cummings, 1984).

2.10. Uronic acid content

Uronic acid content was determined by using aliquots of the sulfuric acid hydrolyzed samples that were used for neutral anhydrocarbohydrate analysis, by an automated *m*-hydroxydiphenyl assay with addition of sodium tetraborate in an autoanalyzer (Skalar Analytical B.V., Breda, The Netherlands). Glucuronic acid was used for calibration.

2.11. Fatty acid extraction and content and compositional analysis by GC–MS

Fatty acids (FA) were extracted according to the protocol from Breuer et al. (2013) and Dodds et al. (2005) with some modifications. C_{D0}-C_{D4} and wheat straw (70 mg), in triplicate, DF_{D0}-DF_{D4} (50 mg), in duplicate, fungal and bacterial controls (2–10 mg) were mixed with 4 mL freshly prepared chloroform:methanol mix (2:2.5 *v*/v) containing an internal standard 1,2-diundecanoyl-sn-glycero-3-phosphocholine (8.5 μg/mL; PC11:0), and sonicated (10 min). Next, 2.5 mL Tris buffer (50 mM Tris, 1 M NaCl, pH 7.5) was added, and samples were vortexed (5 s), sonicated (10 min), and centrifuged (5 min, 1174 xg, 15 °C). The lower biomass-free chloroform phase was carefully transferred to a new tube. The residues were re-extracted 3 times in chloroform (1 mL), by vortexing (5 s) and sonicating (10 min), and centrifuged (5 min, 1174 xg, 15 °C). All chloroform supernatants were pooled and evaporated under a stream of N_2. Methylation was carried out by resolubilizing N_2 dried pellets in toluene (0.3 mL), then methanol (2.7 mL) with 5% H_2SO_4 was added, and samples were incubated (3 h, 70 °C). After cooling to room temperature, milliQ (3 mL) and hexane (3 mL) spiked with 5 μg/mL methyl nonadecanoate (19:0) was added (Dodds et al., 2005). The samples were rotated end-over-end (15 min) and centrifuged (5 min, 1174 xg, 15 °C). A volume of 1 μL of the derivatized sample was injected in a gas chromatograph (Trace1300, Thermo Scientific, Waltham, MA, USA) equipped with a Restek FAMEWAX column (30 m × 0.25 mm id, and film thickness 0.25 μm) coupled to a mass spectrometer MS DCQ II (Thermo Scientific, Waltham, MA, USA). The split injection mode 1:40 was used with the injection port held at 250 °C. The initial oven temperature was set to 150 °C for 2 min, ramped to 250 °C at a rate of 4.0 °C min^{-1}, and held at 250 °C for 3 min. The linear velocity of the carrier gas helium was constant at 1 mL min^{-1}. The MS was operated at positive mode, full scan (*m/z* 50–400) and one of each triplicate was analyzed in full MS mode for correct annotation of fatty acids methyl esters. For quantification selective ion monitoring (SIM) was used to target specific ions for quantification (supplementary material). Peak integration was carried out with a processing method by TraceFinder 4.0 and wrongly integrated peaks were manually corrected. Fatty acid methyl standards (BAME 47080-U, CRM18920, 47,085-U, O7256-1AMP Supelco, Bellefonte, PA, USA) and methyl 12-methyltetradecanoate (*a*-15:0) (Larodan Fine Chemicals AB, Malmö, Sweden) were used for fatty acid annotation. The standards CRM18920 and *a*-15:0 were used quantitatively and used to determine the response factors (RF), by diluting the initial dilution of 0.1 mg/mL 100 fold in 10 steps and spiking the standard with methyl nonadecanoate. Duplicate injections of the dilution series were used to generate individual calibration curves for FAs and were in the range between 0.09 and 0.6 to 9.12–62.4 μg/mL. The averaged slopes of the calibration curves were used as RF. The methyl nonadecanoate was used as a system-check internal standard. Relative response factors (RRF) were calculated by dividing the individual FA response factor by the methyl nonadecanoate response factor. Calibration and calculation of fatty acid content was carried out according to Dodds et al. (2005).

2.12. Lignin analysis by quantitative py-GC–MS

Lignin content and composition analysis was performed as described by van Erven et al. (2019a) without modifications. To each sample, 10 L of uniformly ^{13}C-labeled lignin was added. For a compound list with analyzed pyrolysis products, and the target ions used for quantification, see supplementary material.

2.13. PCR by AusDiagnostics

DNA extracts were analyzed by multiplexed tandem PCR (MT-PCR), using the automated High-Plex 24 PCR system (AusDiagnostics Pty. Ltd., Mascot, New South Wales, Australia) with the MT-Assay Setup Software (Version 1.12.6, AusDiagnostics). A primer panel was especially designed to accurately detect 13 target microorganisms (supplementary material) for tracking maturation of mushroom compost and will be commercially available by AusDiagnostics.

2.14. 16S and 18S rRNA sequencing

The genomic DNA samples were submitted for sequencing to Génome Québec (MacGill University, Montreal, CA) for further details see supplementary material.

2.15. Statistical tests

Technical replicates were averaged, and standard deviations were calculated by excel (Stdev.S). Significance was expressed by a two tailed *p*-value conducting the appropriate *t*-test in excel (t-test, two-sample assuming equal variances or assuming unequal variances based on the F-value).

3. Results and discussion

3.1. Process parameters of wheat straw based microbial composting (PII)

Overall, the temperature in the tunnel increased to 60 °C during the first day (supplementary material). Subsequently, within 3 h hours the temperature decreased to around 45 °C and was kept constant at 45 °C until the end of PII. Besides, a gradual decrease in pH from 8.1 at the start to 7.0 at the end was observed for each bag (supplementary material). Temperature and pH profiles were as expected and previously reported during PII (Jurak et al., 2015).

3.2. Mass flows of wheat straw based microbial composting (PII)

To study the first part of the hypothesis that lignin is degraded throughout the composting PII process, obtained dry matter yields were combined with specific content data to indicate mass flows per component. Analysis of the compost obtained at five timepoints allowed to look into gradual compositional changes throughout PII, while previous research compared only start and end PII compost material (Carrasco et al., 2020; Jurak et al., 2015; Zhang et al., 2019).

These mass flows during PII of moist compost are divided over carbohydrates (cellulose and GAX), lignin, nitrogen, fatty acids, and ash, and presented in Sankey diagrams (Fig. 1). At the start of PII, the tunnel contained 125 tons fresh weight of compost and during the composting a decrease in organic matter (from 25 to 19 tons, Fig. 1, A) and moisture was observed (from 89 to 62 tons; Fig. 1, A), while ash remained constant (11 tons; Fig. 1, A). The fraction specified as 'other' was equal to undefined substances in the dry matter and increased during PII (from 5 to 7 tons; Fig. 1, A). Nitrogen (N) contents were not converted to protein, and a part of 'other' can be certainly assumed to consist of protein. Most likely, in addition, 'other' is (partly) composed of hard-to-quantify microbial cell wall constituents (chitin), degraded wheat-straw biopolymers, and secondary metabolites. Additionally, to a yet undefined extent, degraded organic matter is expected to be scavenged in the form of (supramolecular) associations with a largely hydrophobic, lignin-containing, interior and a more hydrophilic surface (Sutton and Sposito, 2005).

The decrease in organic dry matter was largely related to a 43.7% decrease in carbohydrates (from 14.3 to 8.1 tons, Fig. 1, B), and a 36.3% lignin decrease (from 5.1 to 3.2 tons, Fig. 1, B). The decrease was most pronounced between day 1 and day 2 for carbohydrates, and between day 2 and day 3 for lignin (2.1 tons and 0.8 tons, for carbohydrates and lignin, respectively; Fig. 1, B). A similar decrease in carbohydrates in a comparable PII process (around 50%) was observed in previous studies (Jurak et al., 2015; Zhang et al., 2019). However, other studies found that lignin mostly remained, as mentioned in the above text, which stands in clear contrast with the substantial lignin decrease found in this study (Carrasco et al., 2020; Iiyama et al., 1994; Jurak et al., 2015; Zhang et al., 2019). The reason for this difference is, most likely, related to the applied non-specific gravimetric and spectrophotometric lignin content analyses in previous studies. For example, Jurak et al. (2015) observed only a 10% *w*/w decrease in lignin comparing beginning and end PII compost, which was based on gravimetric Klason lignin quantification. In the same research, it has been shown that with this lignin analysis of a fungal mycelium sample around 50% remained in the Klason residue, indicating the possible overestimation of lignin in compost via this gravimetric determination.

In this study, a recently developed, highly specific lignin quantification method (^{13}C-IS py-GC–MS) was used (van Erven et al., 2017). It has been demonstrated that this ^{13}C-IS py-GC–MS accurately and specifically analyses the lignin content of grasses, e.g. wheat straw, both in

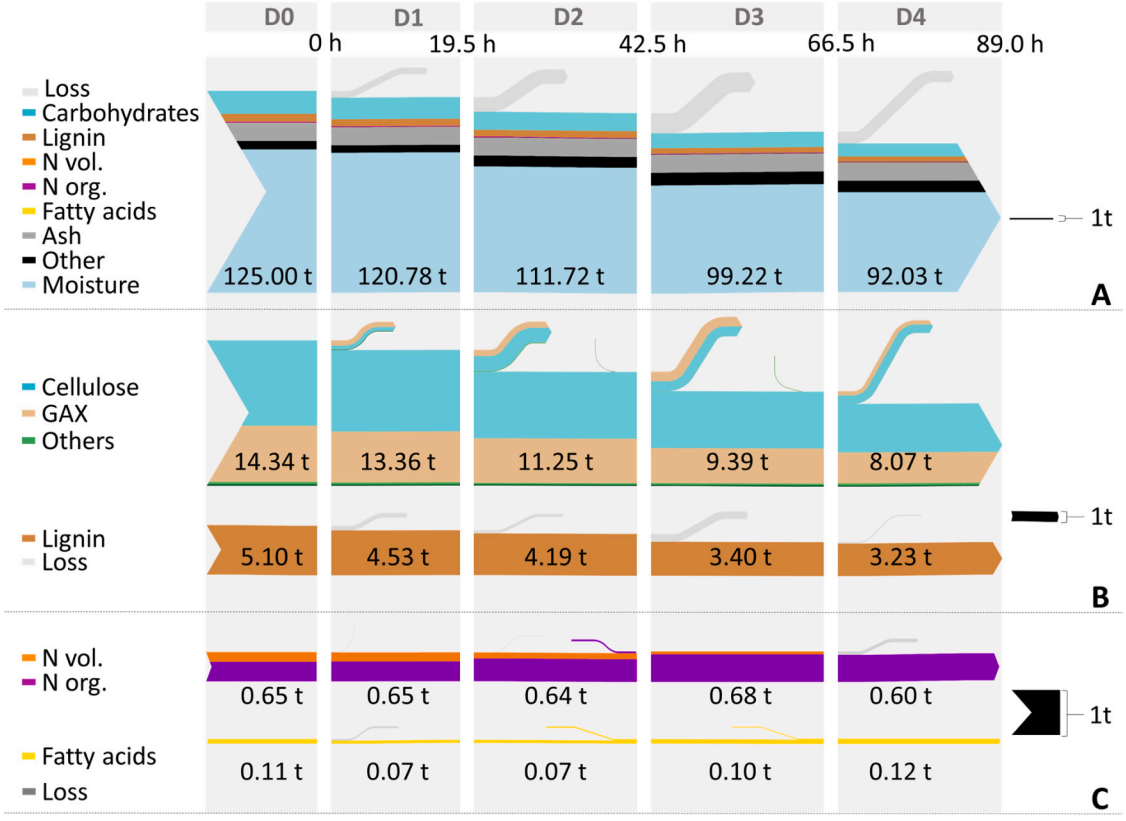

Fig. 1. Sankey diagrams of mass flows during PII: carbohydrates (cellulose – sum of glucosyl residues; GAX ((glucuronoarabino-)xylan) – sum of xylosyl, arabinosyl, uronic acids residues; lignin; nitrogen (vol. – volatile and org. – organic); fatty acids and ash. The arrows' thickness on the right of the diagrams (A, B, C) represents 1 ton (1 t; 1000 kg).

native form as well as in a variety of pretreatment contexts (Hilgers et al., 2020; van Erven et al., 2017). Admittedly, the compost material has a more complex matrix compared to 'pure' wheat straw. In particular H-unit-type pyrolysis products (supplementary material) might partly originate from microbial biomass or protein (i.e., aromatic amino acids (Ralph and Hatfield, 1991)) and not only derive from lignin. Indeed, ^{13}C-IS py-GC–MS analysis of cultivated PII microbial biomass showed a false 'lignin' content of 0.8% (*w*/w) in bacterial and 0.6% (w/w) in fungal biomass, entirely the result of H-unit-pyrolysis compounds (supplementary material). Semi quantification of indole by py-GC–MS in PII samples substantiated the presence of proteinaceous interfering compounds (supplementary material). Therefore, lignin content and composition in the PII samples excluding H-unit-pyrolysis products in ^{13}C-IS and samples (Table 2) were re-analyzed. Doing so for the wheat straw reference sample still gave an accurate, expected lignin content. Based on these data, the lignin content still decreased significantly (*p*-value <0.042) by 36.3% during PII (from 5.1 to 3.2 tons per tunnel) with the most profound decrease (15%) between the second and third day of PII (Fig. 1, B).

The decrease of both carbohydrates and lignin in PII is related to metabolic activity of microbes, which consume compost constituents and produce CO_2 or other volatile compounds (Bernal et al., 2009). It can be assumed that microbial activity drives the observed removal of volatile nitrogen (NH_3; Fig. 1, C), and formation of organic nitrogen. Organic nitrogen increased threefold in content during PII (Fig. 1, C), and most likely, so-called household proteins, protein and amino-sugars present in microbial cell walls and enzymes, were generated. Hence, the observed decrease in C/N ratio, roughly from 15 to 9, is an indication for compost maturation (Paredes et al., 1996).

To get an indication of the extent of microbial biomass formation, fatty acids (FAs) were quantified throughout PII (Fig. 1, C) as microbial plasma membranes are largely built from FAs in form of phospholipids. Although the FA amount in comparison to lignocellulose was low, still, a significant increase from 0.099 tons to 0.126 tons in PII was observed and indicative for the expected increase in microbial biomass. Initial FA contents first dropped from the start till the first day followed by an increase of fatty acids between the second and fourth day of PII. Interestingly, this increase between day 2 and 4 correlated well with the decrease in carbohydrates and lignin, and, again, hints at microbial growth (Fig. 1, C).

3.3. Dynamic changes in carbohydrate and lignin structures during PII

3.3.1. Carbohydrate composition remains stable

Although the major carbohydrates, cellulose and GAX, decreased in amount in PII by 44% and 45%, respectively, the molar carbohydrate composition remained constant (supplementary material). The major part of compost carbohydrates was represented by glucan (55 ± 1 mol%) and GAX (42 ± 1 mol%), and was in the same range as previously reported (Jurak et al., 2015). In compost samples, uronic acids slightly increased during PII (3.9 mol% in C_{D0} to 4.7 mol% in C_{D4}), which might be (partially) due to an analytical interference of microbial biomass. The latter is suggested based on a bacterial control sample (supplementary material) that showed an unusually high uronic acid content. The high uronic acid content was likely the result of colorimetric interference of bacterial muramic acid (Hadžija, 1974). However, uronic acids are part of GAX in compost and even accumulate (Jurak et al., 2015), besides being present in microbial cell wall glycoproteins (Schleifer and Kandler, 1972). Mannosyl residues increased (0.9 mol% in C_{D0} to 1.6 mol% in C_{D4}), which might be related to its accumulation in fungal cell walls in the form of galactomannans or α- and β-mannans (Shibata et al., 2012).

3.3.2. Delignification is substantiated by changes in lignin structure

The delignification during PII, as discussed in Section 3.2, was further substantiated by structural alteration of the residual lignin. Further, to elucidate depolymerized lignin degradation products that became water soluble, water extractable solids (SN_{DO} to SN_{D4}) were analyzed by ^{13}C-IS py-GC–MS. Such water extracts have been previously been characterized to be particularly enriched in compounds that can be used as 'diagnostic structures' to help elucidate and pinpoint the lignin degradation routes that might have taken place (Hilgers et al., 2020; van Erven et al., 2019b).

An overall comparison of the subunit composition showed that S-units were slightly preferentially removed during PII, based on the decreasing percentage of S-units in compost (32.5% in C_{D0} to 29.9% in C_{D4}; Table 1). Consequently, the S/G ratio decreased over time (0.5 to 0.4). The lower redox potential of S-units compared to G-units might result in a preferential removal of these dimethoxylated units from the lignin molecule (Del Río et al., 2002). An opposite effect was found for SN, where the S/G ratio increased throughout the composting phase from 0.3 in SN_{D0} to 0.4 in SN_{D4} (Table 1). This might suggest two potential explanations; either an increased influx of S-units into solution or increased mineralization of solubilized G-units over S-units. In line with the latter observation, it was previously demonstrated that soluble S-units were removed from a bacterial growth medium to a smaller extent than G and H-units (Perez et al., 2019).

A further, more detailed classification and comparison of the detected pyrolysis products revealed additional structural changes during PII. Noteworthy was the significant increase of $C_{\alpha\text{-oxidized}}$compounds from 4.4% in C_{D0} to 5.1% in C_{D4} (*p*-value <0.001) and 4.6% in SN_{D0} to 7.6% in SN_{D4} (p-value <0.01) (Table 1). Especially $C_{\alpha\text{-oxidized}}$ can be associated to occur with cleavage of *β-O*-4 linkages (Bugg et al., 2020). Diketone pyrolysis products were previously identified as diagnostic markers for *O*-4 cleaved *β-O*-4 interunit linkages (van Erven et al., 2019b). Diketones increased analogously in C and in SN from 0.45% in C_{D0} to 0.56% in C_{D4} (*p*-value <0.0003) and even more than twofold from 0.4% in SN_{D0} to 1.1% in SN_{D4} (p-value <0.00004), with the largest increase in SN from the first till the second day of PII (Table 1).

The observed decrease in lignin content in compost during PII and structural alterations discussed above were expected to coincide with a decrease in lignin's interunit linkages. Pyrolysis products with Cγ chains (PhCγ; Table 1) are indicative for intact *β-O*-4 interunit linkages when corrected for diketone pyrolysis products. Diketone pyrolysis products also possess Cγ, but they are formed from cleaved *β-O*-4 units, and thus should be excluded from PhCγ compounds to evaluate intact *β-O*-4 linkages (van Erven et al., 2019b). Indeed, a decline of PhCγ compounds was found, from 55.6% in C_{D0} to 48.1% in C_{D4} (*p*-value <0.0055) (Table 1). However, in SN, PhCγ decreased more strongly from 40.4% in SN_{D0} to 29.8% in SN_{D4} (p-value <0.0008) (Table 1).

3.3.3. Formation of a dark biofilm during microbial composting

Throughout the microbial composting a dark biofilm layer (DF) developed and covered the surface of wheat straw. The DF was isolated by using the newly developed and standardized, polyisoprene assisted protocol (see 2.3). An increased amount of DF was isolated from fresh PII compost of the last two days (C_{D3} and C_{D4}). Thus, isolation yields significantly increased (p-value <0.03) over PII (supplementary material). The most pronounced increase occurred from day two till day three (p-value <0.04). However, yields were lower compared to previous water isolation methods (Iiyami et al., 1996). Though, it is assumed that the here described (2.3) isolation method yielded pure DF due to the mechanic separation technique, compared to Iiyami and colleagues' water extraction, where compounds from wheat-straw are prone to be co-extracted.

Of isolated $DF_{D0\text{-}D4}$ the lignin, carbohydrate, fatty acid, nitrogen (Ntot) and ash contents were determined (dry matter based) (Table.2). The Ntot content dropped from 4.1% in DF_{D0} to 3.3% in DF_{D4} throughout PII. Moreover, the fatty acid, carbohydrate and lignin content and composition of the DF material (DF_{D0}-DF_{D4}) remained constant over PII (% DM based) (Table 2). However, it is doubtful whether the detected lignin in DF should be described as true lignin. Rather, DF's

Table 1
^{13}C-IS py-GC–MS analyzed relative abundances of lignin compounds (RRF corrected) in compost samples (C) and water extracted solids (SN) obtained from PII at the start (D0), after 19.5 h (D1), 42.5 h (D2), 66.5 h (D3), 89 h (D4) excluding H- (phenol) units. Sum on the bases of structural classification (supplementary information). Averages and standard deviation of technical triplicates.

	Compost					Water Extract				
	C_{D0}	C_{D1}	C_{D2}	C_{D3}	C_{D4}	SN_{D0}	SN_{D1}	SN_{D2}	SN_{D3}	SN_{D4}
Lignin content (% w/w)	14.0 ± 0.8	13.3 ± 1.9	12.4 ± 0.8	10.5 ± 0.3	10.7 ± 1.5	6.6 ± 0.8	3.8 ± 0.3	1.9 ± 0.0	1.9 ± 0.1	1.6 ± 0.2
Lignin subunits (%)										
G	67.5 ± 0.5	68.3 ± 0.2	68.5 ± 0.5	69.8 ± 0.3	70.1 ± 0.2	75.8 ± 0.6	79.0 ± 1.7	77.2 ± 0.9	70.0 ± 0.4	70.4 ± 1.3
S	32.5 ± 0.5	31.7 ± 0.2	31.5 ± 0.5	30.2 ± 0.3	29.9 ± 0.2	24.2 ± 0.6	21.0 ± 1.7	22.8 ± 0.9	30.0 ± 0.4	29.6 ± 1.3
S/G	0.5 ± 0.0	0.5 ± 0.0	0.5 ± 0.0	0.4 ± 0.0	0.4 ± 0.0	0.3 ± 0.0	0.3 ± 0.0	0.3 ± 0.0	0.4 ± 0.0	0.4 ± 0.0
Structural moieties (%)										
Unsubstituted	7.5 ± 0.9	7.7 ± 0.7	8.1 ± 0.5	7.6 ± 0.4	8.4 ± 0.6	11.5 ± 0.2	13.3 ± 0.6	14.0 ± 0.4	13.7 ± 0.4	12.4 ± 0.8
Methyl	3.1 ± 0.2	3.5 ± 0.2	3.7 ± 0.3	3.9 ± 0.0	4.2 ± 0.1	2.7 ± 0.1	2.4 ± 0.1	2.4 ± 0.1	2.3 ± 0.1	1.8 ± 0.0
Vinyl	28.7 ± 1.1	30.1 ± 1.3	30.2 ± 0.9	32.0 ± 1.3	33.2 ± 0.5	40.8 ± 0.3	44.2 ± 3.8	45.0 ± 2.9	44.1 ± 0.5	49.1 ± 1.9
4-Vinylguaiacol	24.6 ± 1.0	25.8 ± 1.1	25.8 ± 0.8	27.4 ± 1.1	28.3 ± 0.5	36.6 ± 0.4	40.4 ± 3.6	41.3 ± 2.9	37.0 ± 0.5	40.8 ± 1.6
Cα-ox	4.4 ± 0.1	4.6 ± 0.1	4.6 ± 0.1	5.1 ± 0.1	5.1 ± 0.2	4.6 ± 0.2	5.6 ± 0.6	6.1 ± 0.5	6.4 ± 0.3	7.6 ± 0.6
diketone	0.5 ± 0.0	0.5 ± 0.0	0.5 ± 0.0	0.5 ± 0.0	0.6 ± 0.0	0.4 ± 0.0	0.7 ± 0.1	1.0 ± 0.1	1.1 ± 0.1	1.1 ± 0.0
Cβ-ox	1.4 ± 0.1	1.4 ± 0.0	1.4 ± 0.0	1.4 ± 0.0	1.5 ± 0.0	0.8 ± 0.0	1.0 ± 0.1	1.0 ± 0.1	0.9 ± 0.0	1.0 ± 0.0
Cγ-ox	49.0 ± 2.4	46.2 ± 2.2	45.2 ± 1.7	43.4 ± 2.4	40.4 ± 1.4	37.2 ± 0.8	31.2 ± 4.3	29.2 ± 2.6	30.1 ± 0.7	25.8 ± 2.0
Miscellaneous	5.9 ± 0.3	6.5 ± 0.2	6.9 ± 0.1	6.7 ± 0.6	7.2 ± 0.5	2.4 ± 0.1	2.4 ± 0.2	2.3 ± 0.1	2.4 ± 0.1	2.4 ± 0.2
PhCγ	56.0 ± 2.2	53.8 ± 2.0	53.1 ± 1.6	51.1 ± 1.8	48.7 ± 1.0	40.4 ± 0.7	34.7 ± 4.1	33.1 ± 2.5	34.1 ± 0.5	29.8 ± 1.9
PhCγ (−diketones)	55.6 ± 2.2	53.3 ± 2.0	52.6 ± 1.6	50.6 ± 1.8	48.1 ± 1.0	40.0 ± 0.7	33.9 ± 4.1	32.1 ± 2.5	33.0 ± 0.6	28.7 ± 1.9

Table 2
Dry matter composition (% *w*/w) of DF samples isolated from FC_{D0}, FC_{D1}, FC_{D2}, FC_{D3} and FC_{D4}.

	PII Dark film (DM (% *w*/w))					
	Lignin	Carb.	Lipids	N_{tot}	Ash	Sum
DF_{D0}	6.1 ± 0.2	7.3 ± 0.1	0.7 ± 0.0	4.1 ± 0.0	47.1 ± 0.2	65.3 ± 0.5
DF_{D1}	6.5 ± 0.4	7.8 ± 0.5	0.5 ± 0.0	3.9 ± 0.0	48.6 ± 0.3	67.3 ± 1.2
DF_{D2}	5.2 ± 0.4	7.2 ± 0.2	0.4 ± 0.0	3.5 ± 0.0	51.7 ± 1.4	68.0 ± 2.0
DF_{D3}	4.8 ± 0.5	7.0 ± 0.1	0.4 ± 0.0	3.3 ± 0.0	52.2 ± 0.8	67.7 ± 1.4
DF_{D4}	5.1 ± 0.5	6.7 ± 0.0	0.5 ± 0.0	3.3 ± 0.0	55.6 ± 4.3	71.2 ± 4.8
DM (% w/w), ash corrected						
DF_{D0}	11.4 ± 0.2	13.8 ± 0.1	1.3 ± 0.0	7.8 ± 0.0	n.r.	n.r.
DF_{D1}	12.3 ± 0.4	15.2 ± 0.5	1.0 ± 0.0	7.6 ± 0.0	n.r.	n.r.
DF_{D2}	10.2 ± 0.4	15.0 ± 0.2	0.8 ± 0.0	7.3 ± 0.0	n.r.	n.r.
DF_{D3}	9.7 ± 0.5	14.7 ± 0.1	0.8 ± 0.0	6.9 ± 0.0	n.r.	n.r.
DF_{D4}	11.1 ± 0.5	15.2 ± 0.0	1.1 ± 0.0	7.5 ± 0.0	n.r.	n.r.

lignin should be described as 'lignin-derived degradation products'. Indeed, py-GC–MS analysis of DF showed an evidently different pyrolysis product fingerprint, both compared to native wheat straw and total compost samples. DF was more abundant in unsubstituted and $C\alpha_{ox}$ pyrolysis products and depleted in PhCγ products. These findings support the presence of severely degraded lignin derived compounds (supplementary material).

The fact that around 5% of DF's composition were lignin-like verifies the hypothesis that ligninolytic mechanisms were taking place during PII, since methoxylated lignin-like compounds are not expected to be synthesized *de novo* in DF. The increase in isolated DF towards the end of PII (supplementary material) suggests a specific enrichment with microbial products together with partially degraded wheat-straw carbohydrates, FAs and (degraded) lignin-like compounds. Since DF is known to be removed during *A. bisporus*' mycelial growth, these DF components are expected to be relevant in context of its vegetative growth and a potential nutrient source (Fermor et al., 1991; Iiyami et al., 1996; Smith and Spencer, 1976).

3.3.4. *Tracking selected microbes indicative for compost quality*

Subjecting DNA extracts of C and DF to qPCR allowed to track selected microbes throughout PII composting. Certain microbial targets (e.g., fungal and bacterial) were chosen to track the quality of the compost. *Trichoderma* and *Trichoderma aggressivum*, which are known pathogens, remained undetected as well as *A. bisporus,* as expected (Fig. 2). *Scytalidium thermophilum,* also known as *Mycothermus thermophilus*, is assumed to be beneficial for the composting maturation during PII (Straatsma et al., 1994). The target gene for *M. thermophilus* increased more than 150-fold from C_{D2} to C_{D4} (Fig. 2). As discussed in Section 3.2, FAs are known biomarkers to indicate microbial biomass increase, and a rough classification of FAs present in Gram-positive, Gram-negative and fungal fatty acids can be made (supplementary material). For example, FAs such as linoleic acid and oleic acid can be indicative for fungal biomass (Joergensen and Wichern, 2008), although wheat straw also contains linoleic and oleic acid (Del Río et al., 2013). The high values of oleic acid in compost at the beginning of PII were expected to result from wheat straw in the compost and from microbes from PI (Fig. 3). Still, the sharp increase of FAs from 90 kg on day three to 126 kg on day four of PII compost should relate to an increase of microbial biomass (Fig. 3, A), and particularly the increase of oleic acid (18:1(c/t)) from 19 kg in C_{D0} to 36 kg in C_{D4} (Fig. 3, B) could relate to the observed growth of *M. thermophilus* or other fungal species. Studies revealed a vast enzyme set for cellulose degradation of *M. thermophilus* (Basotra et al., 2016).

The most abundant bacterial group based on qPCR, in compost at the end of PII belonged to Actinomycetales, now named Actinobacteria (Fig. 2). In DF an increase in Actinobacteria was observed, but they were not the most dominant target (Fig. 2). Actinobacteria remained undetected by qPCR in the first half of PII and developed to a dominant target from day two onwards in compost. This increase is in line with previous research where Actinobacteria increased throughout the compost production process (Wang et al., 2016). Actinobacteria are Gram-positive bacteria, their natural habitat is soil and they are important compost microbes (Bhatti et al., 2017). Branched fatty acids such as iso *(i)* and *anteiso (a)* FAs are indicative for Gram-positive bacteria (Williams and Rice, 2007) and indeed in compost analogous of these FAs increased throughout PII (Fig. 3, C). Actinobacteria possess a wide array of enzymes that are involved in delignification, such as peroxidases, polyphenol oxidases and laccases (Kirby, 2005). Actual lignin

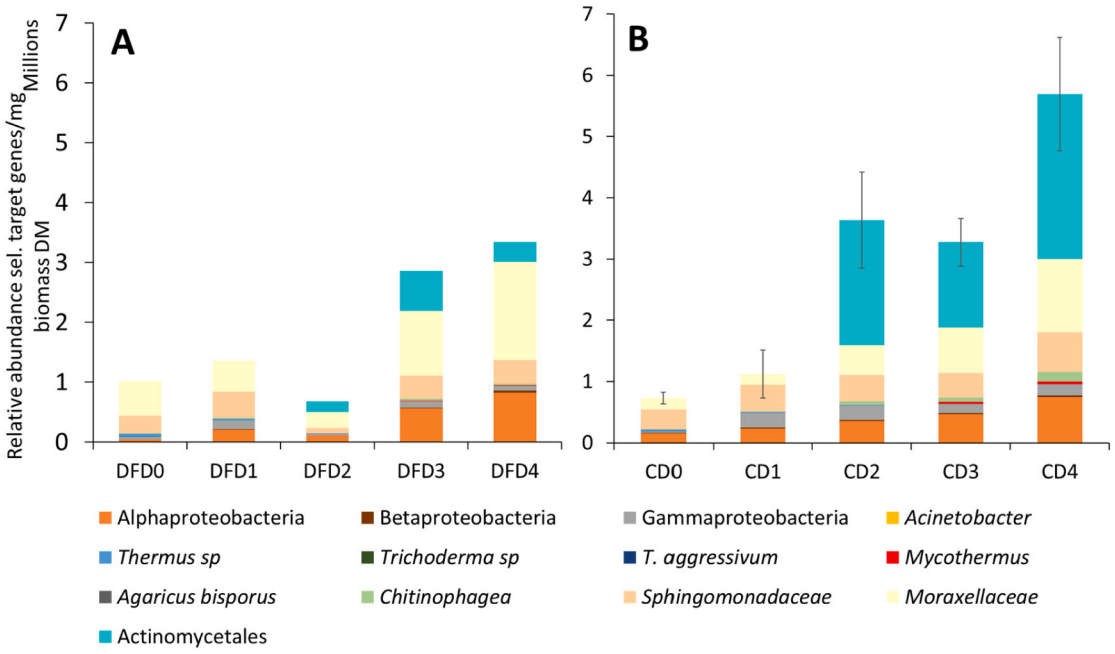

Fig. 2. Relative target gene concentrations of dark film ($DF_{D0\text{-}D4}$ (A)) and compost ($C_{D0\text{-}D4}$ (B)) of selected microbial targets, throughout the production process of composting PII.

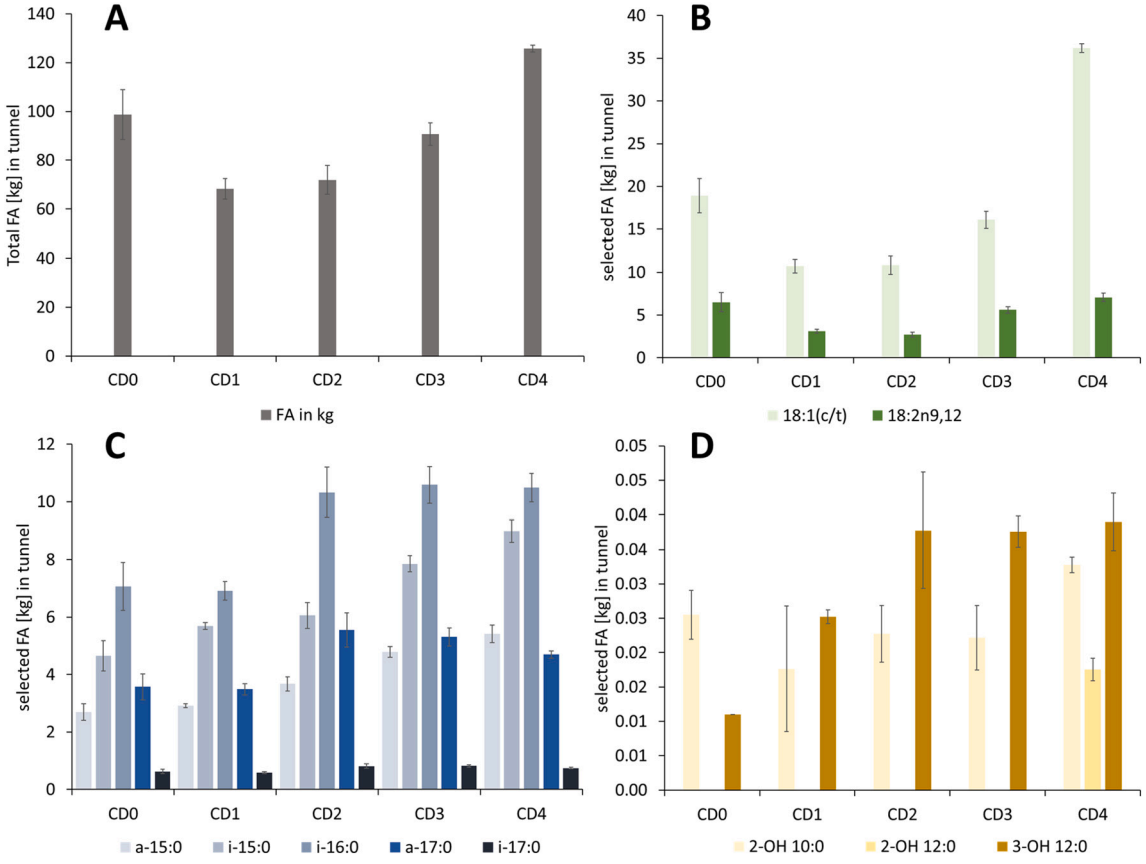

Fig. 3. Fatty acid (FA) amount in kg in tunnel (A) and of selected FA indicative for microbial groups (B, C, D). Branched fatty acids indicative for Gram-positive (C), hydroxylated fatty acids indicative for Gram-negative (D) and selected FA with 18 carbons indicative for fungal biomass (B).

depolymerization has been observed in *Rhodococcus jostii,* a representative of Actinobacteria, by dye decolorizing peroxidases (Bugg et al., 2020). Further, Actinobacteria are known to live in cellulose and hemicellulose rich niches and they can use those polysaccharides as a carbon source (Koeck et al., 2014). Overall, the DF microbial composition followed a similar trend as for the total compost (Fig. 2). However,

it is noteworthy that the Moraxellaceae made up the most dominant target by qPCR in DF. Within the family of Moraxellaceae, certain species have demonstrated to degrade aromatic compounds (van Dexter and Boopathy, 2019) that might hint at the importance of that family in relation to mineralizing lignin degradation products in DF.

3.3.5. *Microbial compositional changes related to ligninolysis*

In context of the delignification observed (see 3.2 and 3.3), the microbial community in compost was studied in more detail. Hereto, DNA extracts from C_{D0} and C_{D4} were sequenced by 16S/18S rRNA. Of the 16 s rRNA sequencing data 100% could be explained on kingdom and phylum level, 98% on class and 94% and order level. Even 86% of the reads could be determined down to family level and 67% to genus level. Solely 9% were described to species level. Of the 18 s rRNA sequencing data 100% could be explained on kingdom, 55% on phylum, 49% on class and 25% and order level. Solely 18% of the reads could be determined down to family level, 17% to genus level and none to species level. Overall, the microbial composition data are in line with literature, which ensured to use the data to compare to the chemical compositional changes observed in compost throughout PII and discussed as such below. Regarding the 16S rRNA sequencing data an increase of diversity could be observed throughout PII, contrary the 18S rRNA data indicated that the diversity decreased throughout PII.

Regarding the 16S rRNA sequencing reads, at phylum level, at the start of PII in C_{D0}, Firmicutes, Deinococcota, Actinobacteria and Proteobacteria were dominant (Fig. 4). At the end of PII, in C_{D4}, Firmicutes and Deinococcota decreased in abundance, while Proteobacteria became most abundant followed by Bacteroidetes (Fig. 4). The occurrence and abundance of these phyla are in line with Carrasco et al. (2020), who observed similar phyla to be the most dominant during PII. Further, Firmicutes, Proteobacteria and Actinobacteria are phyla which are frequently found in organic composting matrices (Jurado et al., 2014; Tortosa et al., 2017). Phylum Deinococcus, known to be extremophile (for example, thermophile), decreased in compost from the start till the end of PII (Fig. 4).

At class level, Bacilli, within the phylum Firmicutes, were the most abundant representatives in the compost, and they decreased in abundance at the end of PII (Fig. 4). This is contrary to Vieira and Pecchia (2018), who observed that Bacilli remained the most abundant order throughout PII. At the end of PII, the Gram-negative bacteria from the classes Gammaproteobacteria, Bacterioidia, and Alphaproteobacteria increased remarkably in compost. Zelles (1999) suggested that Gram-negative bacterial cell walls contain more hydroxylated and cyclopropyl fatty acids. Indeed, hydroxylated FAs increased in compost samples throughout PII (Fig. 3, D). Representatives of the classes Alphaproteobacteria and Gammaproteobacteria are known lignin degraders and some can even further metabolize lignin degradation products (Bugg et al., 2020). For Gammaproteobacteria, especially the well-studied species *Pseudomonas putida* is related with lignin degradation (Salvachúa et al., 2020). *Pseudomonas putida* cleaves aromatic rings via the keto-adipate pathway and possesses peroxidases and multi-copper oxidases involved in delignification (Harwood and Parales, 1996). This exact species was not detected, although an increase in *Pseudomonas* was observed.

Other Gammaproteobacteria, such as *Moraxellaceae* and in particular the genus of *Acetinobacter*, were also more abundant in C_{D4} than C_{D0}. Certain species of *Acetinobacter*, *A. tandoii*, has been associated to phenol removal in termites that funnels phenolic compounds to catechol and further metabolizes this compound (van Dexter and Boopathy, 2019). The last family belonging to Gammaproteobacteria worth mentioning in context to delignification are *Xanthomonadacea*, which increased 30-fold throughout PII. This family has been shown to participate in delignification in forest soil matrices (Wilhelm et al., 2019).

The observed PII delignification could also relate to the increased abundance of Alphaproteobacteria in compost (Figs. 2, 4). In particular, members of the *Sphingomonadaceae* are known to split *β-O*-4 linkages in

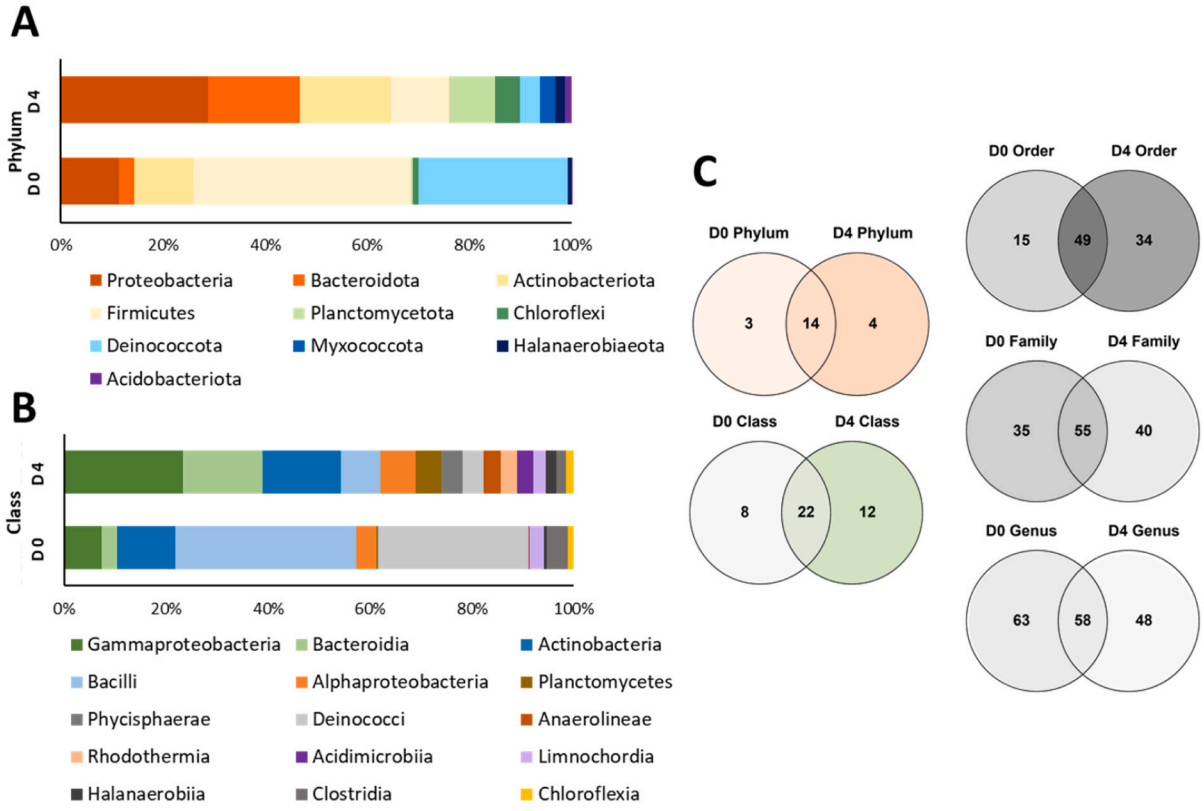

Fig. 4. Bacterial communities in C_{D0} and C_{D4}: the relative abundance of the top 10 phyla (A) and the top 15 bacterial classes (B) using 16S rDNA sequencing (acc. D4). Venn diagrams of C_{D0} and C_{D4} comparing found phyla, classes, orders, families, genera and species.

lignin via their β-etherases pathway (Gall et al., 2014). A myriad of enzymes belonging to the glutathione-S-transferase superfamily are involved in catalyzing β-*O*-4 aryl ether cleavage using glutathione as a cofactor, ultimately yielding hydroxypropiovanillone/syringone substructures (Gall et al., 2014). Upon pyrolysis these structures lead to the formation of acetovanillone/syringone and guaiacol/syringyl vinyl ketone products as previously established by van Erven et al. (2019b). Indeed, in this research the relative abundance of acetovanillone was more than 30% higher in C_{D4} compared to C_{D0}, and in SN a 50% increase was noticed for this compound from SN_{D0} to SN_{D3} with a decrease from SN_{D3} to SN_{D4}. The structural syringyl analogue, acetosyringone, likewise increased in compost throughout PII by 15%, and in SN 40% increased up to day 3, but then largely decreased till the last day of PII. However, both vinyl ketone analogues did not follow the same pattern. Thus, within this research no direct indication of β-etherase activity was found.

18S rRNA data revealed the increase of sequence reads especially of Chaetomium and Verticillium, two genera within the family of Sordariomycetes. The species *Mycothermus thermophilus* (detected by qPCR) also belongs to Cheatomium. Though the relation of the detected Sordariomycetes to delignification remains elusive, still, it is worth mentioning that other members of Sordariomycetes, such as *Podospora anserina*, are known to possess ligninolytic capacities (van Erven et al., 2020). From day 1 to day 4 of PII the diversity of eukaryotic organisms strongly decreased and on the last day of PII solely 14 targets were found by 18S rRNA sequencing, of which 85% of the target reads comprised of the above mentioned two genera.

In general, lignin depolymerization is considered to take place extracellularly, while further degradation and complete mineralization can continue within the cells. However, recently, in Gammaproteobacteria, specifically in *Pseudomonas putida*, outer membrane vesicles (OMVs) have been discovered (Salvachúa et al., 2020). These OMVs are found to contain an enzyme toolkit to degrade lignin building blocks, and can travel from the outside of the microbial cells to the target, where they release the transported enzymes (Salvachúa et al., 2020). Whether such OMVs could play a role in PII composting has yet to be defined, but it might explain how enzymes could successfully access the complex compost matrix to reach the rather high delignification observed.

4. Conclusion

This research provides compelling evidence that lignin decreased and got structurally modified during phase II of an industrial mushroom substrate production process, by relying on a specific lignin quantification method (i.e., pyrolysis-GC–MS using ^{13}C-lignin as internal standard). A 30% *w*/w lignin decrease was found, which was linked to potential delignification routes and relevant ligninolytic bacteria present in the compost were identified. Dark film was compositionally elucidated and was partly composed of lignin-like structures and microbial biomass. The results imply that oxidative ligninolysis cascades underly delignification, which in broad context matches the capabilities of the microbial community present during PII.

CRediT authorship contribution statement

Katharina Duran: Conceptualization, Formal analysis, Methodology, Investigation, Visualization, Writing – original draft. **Marijn van den Dikkenberg:** Visualization, Formal analysis. **Gijs van Erven:** Methodology, Validation, Writing – review & editing. **Johan J.P. Baars:** Conceptualization, Resources, Writing – review & editing. **Rob N.J. Comans:** Conceptualization, Writing – review & editing, Supervision. **Thomas W. Kuyper:** Conceptualization, Writing – review & editing, Supervision. **Mirjam A. Kabel:** Conceptualization, Validation, Methodology, Writing – review & editing, Supervision.

Declaration of competing interest

The authors declare that they have no known competing financial interests or personal relationships that could have appeared to influence the work reported in this paper.

Acknowledgments

The authors thank Tânia V. Fernandes and Lukas M. Trebuch (NIOO-KNAW) for helping with 16S and 18S rRNA sequencing. This research received funding from The Netherlands Organization for Scientific Research (NWO) by an NWO Graduate School Green Top Sector grant (GSGT.GSGT. 2018.0 18), which is conducted in collaboration with CNC Grondstoffen and IsoLife.

Appendix A. Supplementary data

Supplementary data to this article can be found online at https://doi.org/10.1016/j.biteb.2021.100911.

References

Albrecht, R., Ziarelli, F., Alarcón-Gutiérrez, E., Le Petit, J., Terrom, G., Perissol, C., 2008. 13C solid-state NMR assessment of decomposition pattern during co-composting of sewage sludge and green wastes. Eur. J. Soil Sci. 59, 445–452. https://doi.org/10.1111/J.1365-2389.2007.00993.X.

Basotra, N., Kaur, B., Di Falco, M., Tsang, A., Chadha, B.S., 2016. Mycothermus thermophilus (Syn. Scytalidium thermophilum): repertoire of a diverse array of efficient cellulases and hemicellulases in the secretome revealed. Bioresour. Technol. 222, 413–421. https://doi.org/10.1016/j.biortech.2016.10.018.

Bernal, M.P., Alburquerque, J.A., Moral, R., 2009. Composting of animal manures and chemical criteria for compost maturity assessment. A review. Bioresour. Technol. 100, 5444–5453. https://doi.org/10.1016/j.biortech.2008.11.027.

Bhatti, A.A., Haq, S., Bhat, R.A., 2017. Actinomycetes benefaction role in soil and plant health. Microb. Pathog. https://doi.org/10.1016/j.micpath.2017.09.036.

Breuer, G., Evers, W.A.C., de Vree, J.H., Kleinegris, D.M.M., Martens, D.E., Wijffels, R.H., Lamers, P.P., 2013. Analysis of fatty acid content and composition in microalgae. J. Vis. Exp. 1–8 https://doi.org/10.3791/50628.

Bugg, T.D.H., Williamson, J.J., Rashid, G.M.M., 2020. Bacterial enzymes for lignin depolymerisation: new biocatalysts for generation of renewable chemicals from biomass. Curr. Opin. Chem. Biol. 55, 26–33. https://doi.org/10.1016/j.cbpa.2019.11.007.

Carrasco, J., García-Delgado, C., Lavega, R., Tello, M.L., De Toro, M., Barba-Vicente, V., Rodríguez-Cruz, M.S., Sánchez-Martín, M.J., Pérez, M., Preston, G.M., 2020. Holistic assessment of the microbiome dynamics in the substrates used for commercial champignon (Agaricus bisporus) cultivation. Microb. Biotechnol. 1751–7915, 13639. https://doi.org/10.1111/1751-7915.13639.

Chen, Y., Inbar, Y., Hadar, Y., Malcolm, R.L., 1989. Chemical properties and solid-state CPMAS 13C-NMR of composted organic matter. Sci. Total Environ. 81–82, 201–208. https://doi.org/10.1016/0048-9697(89)90126-5.

Del Río, J.C., Speranza, M., Gutiérrez, A., Martínez, M.J., Martínez, A.T., 2002. Lignin attack during eucalypt wood decay by selected basidiomycetes: a Py-GC/MS study. J. Anal. Appl. Pyrolysis 64, 421–431. https://doi.org/10.1016/S0165-2370(02)00043-8.

Del Río, J.C., Prinsen, P., Gutiérrez, A., 2013. A comprehensive characterization of lipids in wheat straw. J. Agric. Food Chem. 61, 1904–1913. https://doi.org/10.1021/jf304252m.

van Dexter, S., Boopathy, R., 2019. Biodegradation of phenol by Acinetobacter tandoii isolated from the gut of the termite. Environ. Sci. Pollut. Res. 26, 34067–34072. https://doi.org/10.1007/s11356-018-3292-4.

Dodds, E.D., McCoy, M.R., Rea, L.D., Kennish, J.M., 2005. Gas chromatographic quantification of fatty acid methyl esters: flame ionization detection vs. electron impactmass spectrometry. Lipids 40, 419–428. https://doi.org/10.1007/s11745-006-1399-8.

Englyst, H.N., Cummings, J.H., 1984. Simplified method for the measurement of total non-starch polysaccharides by gas - liquid chromatography of constituent sugars as alditol acetates. Analyst 109, 937–942. https://doi.org/10.1039/an9840900937.

van Erven, G., De Visser, R., Merkx, D.W.H., Strolenberg, W., De Gijsel, P., Gruppen, H., Kabel, M.A., 2017. Quantification of lignin and its structural features in plant biomass using 13C lignin as internal standard for pyrolysis-GC-SIM-MS. Anal. Chem. 89, 10907–10916. https://doi.org/10.1021/acs.analchem.7b02632.

van Erven, G., De Visser, R., De Waard, P., van Berkel, W.J.H., Kabel, M.A., 2019. Uniformly 13C labeled lignin internal standards for quantitative pyrolysis-GC-MS analysis of grass and wood. ACS Sustain. Chem. Eng. https://doi.org/10.1021/acssuschemeng.9b05926.

van Erven, G., Hilgers, R., de Waard, P., Gladbeek, E.J., van Berkel, W.J.H., Kabel, M.A., 2019b. Elucidation of in situ ligninolysis mechanisms of the selective white-rot fungus Ceriporiopsis subvermispora. ACS Sustain. Chem. Eng. 7 https://doi.org/10.1021/acssuschemeng.9b04235.

van Erven, G., Kleijn, A.F., Patyshakuliyeva, A., Di Falco, M., Tsang, A., De Vries, R.P., van Berkel, W.J.H., Kabel, M.A., 2020. Evidence for ligninolytic activity of the ascomycete fungus Podospora anserina. Biotechnol. Biofuels 13. https://doi.org/10.1186/s13068-020-01713-z.

Fermor, T.R., Wood, D.A., Lincoln, S.P., Fenlon, J.S., 1991. Bacteriolysis by Agaricus bisporus. J. Gen. Microbiol. 137, 15–22. https://doi.org/10.1099/00221287-137-1-15.

Gall, D.L., Ralph, J., Donohue, T.J., Noguera, D.R., 2014. A group of sequence-related sphingomonad enzymes catalyzes cleavage of β-aryl ether linkages in lignin β-guaiacyl and β-syringyl ether dimers. Environ. Sci. Technol. 48, 12454–12463. https://doi.org/10.1021/es503886d.

Gírio, F.M., Fonseca, C., Carvalheiro, F., Duarte, L.C., Marques, S., Bogel-Łukasik, R., 2010. Hemicelluloses for fuel ethanol: a review. Bioresour. Technol. https://doi.org/10.1016/j.biortech.2010.01.088.

Hadžija, O., 1974. A simple method for the quantitative determination of muramic acid. Anal. Biochem. 60, 512–517. https://doi.org/10.1016/0003-2697(74)90261-9.

Harwood, C.S., Parales, R.E., 1996. Harwood, C. S., & Parales, R. E. (1996). The β-ketoadipate pathway and the biology of self-identity. Annu. Rev. Microbiol. 50, 553–590. https://doi.org/10.1146/annurev.micro.50.1.553.

Hilgers, R., van Erven, G., Boerkamp, V., Sulaeva, I., Potthast, A., Kabel, M.A., Vincken, J.P., 2020. Understanding laccase/HBT-catalyzed grass delignification at the molecular level. Green Chem. 22, 1735–1746. https://doi.org/10.1039/c9gc04341a.

Iiyama, K., Stone, B.A., Macauley, B.J., 1994. Compositional changes in compost during composting and growth of Agaricus bisporus. Appl. Environ. Microbiol. 60, 1538–1546.

Iiyami, K., Lam, T.B.T., Stone, B.A., Macauley, B.J., 1996. Characterisation of material generated on the surface of wheat straw during composting for mushroom production. J. Sci. Food Agric. 70, 461–467. https://doi.org/10.1002/(SICI)1097-0010(199604)70:4<461::AID-JSFA501>3.3.CO;2-W.

Joergensen, R.G., Wichern, F., 2008. Quantitative assessment of the fungal contribution to microbial tissue in soil. Soil Biol. Biochem. 40, 2977–2991. https://doi.org/10.1016/j.soilbio.2008.08.017.

Jurado, M., López, M.J., Suárez-Estrella, F., Vargas-García, M.C., López-González, J.A., Moreno, J., 2014. Exploiting composting biodiversity: Study of the persistent and biotechnologically relevant microorganisms from lignocellulose-based composting. Bioresour. Technol. 162, 283–293. https://doi.org/10.1016/j.biortech.2014.03.145.

Jurak, E., Punt, A.M., Arts, W., Kabel, M.A., Gruppen, H., 2015. Fate of carbohydrates and lignin during composting and mycelium growth of agaricus bisporus on wheat straw based compost. PLoS One 10, e0138909. https://doi.org/10.1371/journal.pone.0138909.

Kabel, M.A., Jurak, E., Mäkelä, M.R., de Vries, R.P., 2017. Occurrence and function of enzymes for lignocellulose degradation in commercial Agaricus bisporus cultivation. Appl. Microbiol. Biotechnol. 101, 4363–4369. https://doi.org/10.1007/s00253-017-8294-5.

Kertesz, M.A., Thai, M., 2018. Compost bacteria and fungi that influence growth and development of Agaricus bisporus and other commercial mushrooms. Appl. Microbiol. Biotechnol. https://doi.org/10.1007/s00253-018-8777-z.

Kirby, R., 2005. Actinomycetes and lignin degradation. Adv. Appl. Microbiol. https://doi.org/10.1016/S0065-2164(05)58004-3.

Koeck, D.E., Pechtl, A., Zverlov, V.V., Schwarz, W.H., 2014. Genomics of cellulolytic bacteria. Curr. Opin. Biotechnol. https://doi.org/10.1016/j.copbio.2014.07.002.

Meghvansi, M.K., Varma, A., 2020. Biology of Composts. Springer.

Paredes, C., Bernal, M.P., Cegarra, J., Roig, A., Navarro, A.F., 1996. Nitrogen tranformation during the composting of different organic wastes. In: Progress in Nitrogen Cycling Studies. Springer, Netherlands, pp. 121–125. https://doi.org/10.1007/978-94-011-5450-5_19.

Patyshakuliyeva, A., Post, H., Zhou, M., Jurak, E., Heck, A.J.R., Hildén, K.S., Kabel, M.A., Mäkelä, M.R., Altelaar, M.A.F., de Vries, R.P., 2015. Uncovering the abilities of Agaricus bisporus to degrade plant biomass throughout its life cycle. Environ. Microbiol. 17, 3098–3109. https://doi.org/10.1111/1462-2920.12967.

Perez, J.M., Kontur, W.S., Alherech, M., Coplien, J., Karlen, S.D., Stahl, S.S., Donohue, T. J., Noguera, D.R., 2019. Funneling aromatic products of chemically depolymerized lignin into 2-pyrone-4-6-dicarboxylic acid with Novosphingobium aromaticivorans. Green Chem. 21, 1340–1350.

Ralph, J., Hatfield, R., 1991. Pyrolysis-GC-MS characterization of forage materials. J. Agric. Food Chem. 39, 1426–1437. https://doi.org/10.1021/jf00008a014 M4 - Citavi.

Ralph, J., Lundquist, K., Brunow, G., Lu, F., Kim, H., Schatz, P.F., Marita, J.M., Hatfield, R.D., Ralph, S.A., Christensen, J.H., Boerjan, W., 2004. Lignins: natural polymers from oxidative coupling of 4-hydroxyphenyl- propanoids. Phytochem. Rev. 3, 29–60. https://doi.org/10.1023/B:PHYT.0000047809.65444.a4.

Salvachúa, D., Werner, A.Z., Pardo, I., Michalska, M., Black, B.A., 2020. Outer Membrane Vesicles Catabolize Lignin-derived Aromatic Compounds in Pseudomonas putida KT2440. https://doi.org/10.1073/pnas.1921073117.

Schleifer, K.H., Kandler, O., 1972. Peptidoglycan types of bacterial cell walls and their taxonomic implications. Bacteriol. Rev. 36, 407–477.

Shibata, N., Kobayashi, H., Suzuki, S., 2012. Immunochemistry of pathogenic yeast, Candida species, focusing on Mannan. Proc. Jpn. Acad. Ser. B Phys. Biol. Sci. https://doi.org/10.2183/pjab.88.250.

Siyoum, N.A., Surridge, K., van der Linde, E.J., Korsten, L., 2016. Microbial succession in white button mushroom production systems from compost and casing to a marketable packed product. Ann. Microbiol. 66, 151–164. https://doi.org/10.1007/s13213-015-1091-4 M4 - Citavi.

Smith, J.F., Spencer, D.M., 1976. Rapid preparation of composts suitable for the production of the cultivated mushroom. Sci. Hortic. (Amsterdam) 5, 23–31. https://doi.org/10.1016/0304-4238(76)90019-4.

Straatsma, G., Olijnsma, T.W., Gerrits, J.P.G., Amsing, J.G.M., Op Den Camp, H.J.M., van Griensven, L.J.L.D., 1994. Inoculation of Scytalidium thermophilum in button mushroom compost and its effect on yield. Appl. Environ. Microbiol. 60, 3049–3054. https://doi.org/10.1128/aem.60.9.3049-3054.1994.

Sutton, R., Sposito, G., 2005. Molecular structure in soil humic substances: the new view. Environ. Sci. Technol. https://doi.org/10.1021/es050778q.

Tortosa, G., Castellano-Hinojosa, A., Correa-Galeote, D., Bedmar, E.J., 2017. Evolution of bacterial diversity during two-phase olive mill waste (“alperujo”) composting by 16S rRNA gene pyrosequencing. Bioresour. Technol. 224, 101–111. https://doi.org/10.1016/j.biortech.2016.11.098.

Tuomela, M., 2000. Biodegradation of lignin in a compost environment: a review. Bioresour. Technol. 72, 169–183. https://doi.org/10.1016/S0960-8524(99)00104-2 M4 - Citavi.

Vieira, F.R., Pecchia, J.A., 2018. An exploration into the bacterial community under different pasteurization conditions during substrate preparation (composting–phase II) for Agaricus bisporus cultivation. Microb. Ecol. 75, 318–330. https://doi.org/10.1007/s00248-017-1026-7.

Wain, D.I., 1981. Investigation of the Nutrition of the Mushroom Agaricus bisporus (Lange.) Sing. in Compost.

Wang, L., Mao, J., Zhao, H., Li, M., Wei, Q., Zhou, Y., Shao, H., 2016. Comparison of characterization and microbial communities in rice straw- and wheat straw-based compost for Agaricus bisporus production. J. Ind. Microbiol. Biotechnol. 43, 1249–1260. https://doi.org/10.1007/s10295-016-1799-6.

Wilhelm, R.C., Singh, R., Eltis, L.D., Mohn, W.W., 2019. Bacterial contributions to delignification and lignocellulose degradation in forest soils with metagenomic and quantitative stable isotope probing. ISME J. 13, 413–429. https://doi.org/10.1038/s41396-018-0279-6.

Williams, M.A., Rice, C.W., 2007. Seven years of enhanced water availability influences the physiological, structural, and functional attributes of a soil microbial community. Appl. Soil Ecol. 35, 535–545. https://doi.org/10.1016/j.apsoil.2006.09.014.

Zelles, L., 1999. Fatty acid patterns of phospholipids and lipopolysaccharides in the characterisation of microbial communities in soil: a review. Biol. Fertil. Soils 29, 111–129. https://doi.org/10.1007/s003740050533 M4 - Citavi.

Zhang, H.-L., Wei, J.-K., Wang, Q.-H., Yang, R., Gao, X.-J., Sang, Y.-X., Cai, P.-P., Zhang, G.-Q., Chen, Q.-J., 2019. Lignocellulose utilization and bacterial communities of millet straw based mushroom (*Agaricus bisporus*) production. Sci. Rep. 9, 1151. https://doi.org/10.1038/s41598-018-37681-6.